Slow relaxation in weakly open rational polygons

Valery B. Kokshenev[1] and Eduardo Vicentini[2]
[1]*Departamento de Física, Universidade Federal de Minas Gerais, ICEx, Caixa Postal 702, CEP 30123-970, Belo Horizonte, Minas Gerais, Brazil*
[2]*Departamento de Física, Universidade Estadual do Centro Oeste, Caixa Postal 730, CEP 85010-990, Guarapuara, Paraná, Brazil*
(Received 14 August 2002; published 31 July 2003)

The interplay between the regular (piecewise-linear) and irregular (vertex-angle) boundary effects in nonintegrable rational polygonal billiards (of m equal sides) is discussed. Decay dynamics in polygons (of perimeter P_m and small opening Δ) is analyzed through the late-time survival probability $S_m \sim t^{-\delta}$. Two distinct slow relaxation channels are established. The primary universal channel exhibits relaxation of regular sliding orbits, with $\delta=1$. The secondary channel is given by $\delta>1$ and becomes open when $m>P_m/\Delta$. It originates from vertex order-disorder dual effects and is due to relaxation of chaoticlike excitations.

DOI: 10.1103/PhysRevE.68.016221 PACS number(s): 05.45.Gg, 45.50.Tn, 05.40.Fb

I. INTRODUCTION

Classical polygonal billiards is an active subject of research in mathematics and physics (see Ref. [1] for review). In view of their null Lyapunov exponent and null Kolmogorov metric entropy, rational polygons, formed by the piecewise-linear billiard boundary with the vertex angles that are rational multiplies of π, are known to be *nonchaotic* systems [1–6]. They are therefore quite distinct from the Sinai billiard (SB) [7] and the Bunimovich billiard (BB) [8] in which classical *chaotic* motion regimes are due to, respectively, *dispersive* effects caused by the disk and the square boundary, and the *interplay* between boundary segments formed by the circle and the square. Rational polygons of m equal sides and m equal vertices (hereafter, m-gons [1]) have been shown [9] however to possess positive Lyapunov exponents with increasing m. Furthermore, polygonal billiards exhibit chaoticlike changes in the associated quantum-level spectra [10], the fluctuations of which are found [11,12] to be very close to the standard Gaussian statistics. These chaoticlike features are due to the *splitting* effects caused by the angle vertices. Vertex-splitting effects, even being related to zero-measure singularities in phase space, violate the integrability of polygons, [2,13] as well as the classical-to-quantum correspondence principle [6] for chaotic billiards geometrically approximated (quantized) by polygons. The latter was recently reported by Mantica [6], who found a logarithmically divergent contribution by vertices to the algorithmic complexity of symbolic trajectories. As to nonchaotic systems, exemplified by circle billiard (CB) and analyzed through the average coding length, it was argued [6] that the correspondence principle between the classical integrable CB and its nonintegrable m-gonal quantum counterpart is valid when $m\to\infty$.

The delicate interplay between the regular (piecewise-linear) and the irregular (vertex-angle) boundary segments in polygons provides interesting features that cannot be understood solely in terms of the averaged temporal and spatial polygonal characteristics. Besides the chaoticlike effects, there were attempts to find long-range correlations in the orbit-length [14] and quantum-level [11] spectral characteristics of rational and irrational polygons. The orbit-wall-collision statistics [15,16] applied to m-gons [17] revealed the late-time memory effects driven by long-lived *sliding orbits*. These orderlike orbits show regular (mean) and anomalous (root-mean-square) wall-collision behavior, which is responsible for superdiffusive *intrinsic dynamics* [17] in rational polygons with large numbers of sides m. The sliding orbits in the infinite-m polygon (∞-gon) has no analog in the ballistic dynamics of its counterpart given by the CB, where the orbit classification is well established [18]. The *dynamic correspondence* found [6] between a given m-gon and the CB is therefore violated by sliding orbits (see Fig. 1 in Ref. [17]) despite the existence of *geometric correspondence*, which can be controlled via the concept of averaged characteristics (such as mean collision time [17] or averaged coding length [6]) with arbitrary precision when $m\to\infty$ (see Fig. 4 in Ref. [6]). This finding is in line with a conclusion on inapplicability in polygons of the quantum-to-classical correspondence elaborated [12] within the scope of the conventional Wentzell-Kramer-Brillouin picture, which fails to establish a one-to-one correspondence between classical orbits and their quantum counterparts.

The objective of the present paper is a further investigation of memory effects induced by sides and vertices in rational finite-m weakly open polygons, in which the boundaries permit orbits to escape through a small opening. We will show that the sliding orbits, responsible for the enhanced diffusive regime in the intrinsic dynamics [17] of closed m-gons, give rise to qualitatively new vertex-correlation effects in late-time decay dynamics. For certain geometrical conditions, the sliding orbits generate vortexlike excitations, which remain stable in large-m rational polygons and provide a specific channel of relaxation common to chaotic billiards. The paper is organized as follows. Decay dynamics in chaotic and nonchaotic billiards is reviewed in Sec. II, within the context of distinct channels of relaxation. Weakly open rational polygons are analyzed numerically and analytically in Sec. III for the cases of small and large numbers m. Summary and conclusions are given in Sec. IV.

II. DECAY DYNAMICS OF CHAOTIC AND NONCHAOTIC BILLIARDS

The intrinsic dynamics of closed classical billiards is commonly discussed in terms of a temporal decay of corre-

lation functions for certain dynamical variables (see, e.g., Ref. [19]). A pure exponential loss of an amount of memory of the initial state is not a unique channel of relaxation even in chaotic systems (see, e.g., Ref. [20]). By studying chaotic billiards, such as the SB [20–23], that is dynamically equivalent to the Lorentz gas (LG) with a corresponding geometry [19] and the BB [8,24,25], it has been recognized that a crossover from the short-time exponential to the late-time algebraic decay is due to long-term memory on a regular-orbit motion. The algebraic tail of the correlation functions seems to vanish only in the case of completely hyperbolic systems which correspond to geometries such as the finite-horizon SB [19,22] (equivalent to the high-density LG) or the diamond billiard [19]. Qualitatively, the same can be asserted for the decay dynamics in weakly open billiards which describes a crossover from a bounded to an unbounded free motion of orbits. Such a decay dynamics is initially established by $N(0)$ uniformly distributed point particles (of unit mass and unit velocity) moving inside the closed planar billiard table, which are allowed to escape through a small opening of width Δ. A temporal behavior of the dynamic observables can be scaled to the characteristic billiard times. These are *mean collision time* [19,26,27] τ_c and the *mean escape time* [16,19,24,28] τ_e, namely,

$$\tau_c = \frac{\pi A}{P} \quad \text{and} \quad \tau_e = \frac{P}{\Delta}\tau_c, \tag{1}$$

given through the accessible area A and the perimeter P ($\gg\Delta$) for a billiard table. The late-time evolution of $N(t)$ nonescaped orbits (particles) provides an asymptotic behavior of the billiard *survival probability* $S(t)$, which is definitely characterized by the algebraic-decay *dynamic exponent* δ:

$$S(t) = \frac{N(t)}{N(0)} \propto \left(\frac{\tau_e}{t}\right)^{\delta} \quad \text{for } t \gg \tau_e. \tag{2}$$

For the nonchaotic square billiard, the algebraic decay with exponents $\delta \lessapprox 1$ was reported in Ref. [28]. In a careful study of the decay dynamics in the integrable CB, the almost integrable [1] 4-gon established [16] two distinct channels of algebraic slow relaxation given in Eq. (2). The first is due to the regular-orbit motion with the decay exponent $\delta=1$ and the second channel originates from irregular orbits, which give rise to a subdiffusive regime indicated [16] for the square billiard by $\delta<1$. The irregular-orbit motion is known in both cases. For the CB and the 4-gon, this is due to the short-lived whispering-gallery and long-lived bouncing-ball orbits, respectively. Nevertheless, the short-lived orbits do not contribute to the second channel of late-time relaxation, and therefore only a unique decay exponent $\delta=1$ is observed [16] in the integrable case.

In chaotic closed and weakly open classical systems (including Hamiltonian systems), exemplified by the BB [24,25,29,30], the infinite-horizon SB [15,20,21,23,31,32], and the corresponding low-density LG [22,33,34], the overall algebraic decay was found numerically with the geometry-dependent exponents $\delta \gtrsim 1$. Similar to the nonchaotic case, it has been repeatedly recognized that the algebraic tail is caused by the ''arbitrary long segments,'' observed in the evolution of stochastic orbits [25], or by the regular-orbit motion due to ''sticking particles'' [30,35]. This implies that relaxation given in Eq. (2) is due to free motion of the corresponding trajectories in the infinite distinct *corridors* which are accessible in the relevant phase space [31–33]. The algebraic-relaxation channel with $\delta=1$ (hereafter, α-relaxation channel) established in chaotic [15,20,24,31,32] as well as in nonchaotic [16,28] billiards appears to be generic for all incompletely hyperbolic systems with smooth convex boundaries. The independence with respect to the billiard spatial dimension [32], its insensitivity to details of the boundary shape [16], including a location of a small opening [24], and to the initial conditions [16] suggests that late-time α relaxation arises in classical systems as a *universal primary relaxation*.

In chaotic [15] and nonchaotic [16] weakly open classical systems, slow α relaxation is a part of the universal two-step relaxation scenario consisting of the short-time pure exponential decay, $S(t) \propto e^{-(t/\tau_e)^{\gamma}}$, with $\gamma=1$, and the late-time algebraic decay, with $\delta=1$. This scenario follows from the billiard survival probability found [15,16] in explicit form, namely,

$$S(t) = \frac{\operatorname{erf}\left(\frac{t}{\tau_{e2}} + \frac{\tau_{e1}}{\tau_{e2}}\right) - \operatorname{erf}\left(\frac{t}{\tau_{e2}} - \frac{\tau_{e1}}{\tau_{e2}}\right)}{2\operatorname{erf}\left(\frac{\tau_{e1}}{\tau_{e2}}\right)} \times \exp\left[\frac{t}{\tau_{e2}}\left(\frac{t}{\tau_{e2}} - 2\frac{\tau_{e1}}{\tau_{e2}}\right)\right], \tag{3}$$

where $\operatorname{erf}(x)$ is the standard error function. The characteristic times τ_{e1}, τ_{e2} ($\sim\tau_e$), which depend crucially on specific billiard geometry, establish temporal observation conditions (hereafter, *observation windows*): $0 \leqslant t < \min(\tau_{e1}, \tau_{e2})$ and $\max(\tau_{e1}, \tau_{e2}) < t < t_{\max}$, respectively, for the universal $\gamma=1$-exponential and $\delta=1$-algebraic channels of relaxation. The upper limit of the α-relaxation observation window $t_{\max}$ was defined analytically [15,16] and numerically [16], but there are certain geometrical situations when this window disappears [31,36]. Keeping in mind that the explicit form of $S(t)$ is deduced from the fundamental decay-kinetics equation under general Gaussian-escape-mechanism assumptions [15,16], it seems plausible that the universal decay of two-dimensional (2D) classical systems can be given by a generic form of Eq. (3) with specific parameters τ_{e1} and τ_{e2}, which can be established, similar to chaotic [15] and nonchaotic [16] cases. It is noteworthy that in the context of exactly solvable 1D random walks, a slow universal relaxation with $S(t) \propto t^{-1}$ emerges [37,38] as history-dependent steps with an absorbing origin in the presence of an ideal reflector, which play the role of billiard opening and regular boundary, respectively.

A survival probability for the intermediate, *nonuniversal* transient regime also follows from Eq. (3), which was approximated by a stretched-exponential form [15] with $\gamma<1$, studied earlier analytically [39] and numerically [19] in chaotic billiards. Other nonuniversal algebraic decays with

$\delta \neq 1$ were explored in Refs. [20,24,31,32,37,38]. Unlike the case of primary relaxation, the *secondary relaxation* in chaotic billiards with ($\beta=$) $\delta>1$ (hereafter, β relaxation) is shown to be very sensitive to the billiard geometry [16], the dimension [32] d of a billiard table, and the initial conditions [16]. This can be exemplified by the dynamic-exponent constraint $1<\beta\leqslant d$ proposed in Ref. [32] and observed in the chaotic BB [24] and SB [20,31,32]. For $d=1$, this regime corresponds to an unbiased random walk in a ''hostile environment'' [38].

One can see that incomplete hyperbolic billiards, on one hand, are indiscernible from their decay dynamics, observed solely through the primary universal α-relaxation channel. On the other hand, chaotic and nonchaotic weakly open billiards are well distinguished with respect to nonuniversal relaxations through the continuously variable [38] dynamic exponents $\beta>1$ and $\delta<1$, respectively. In what follows, we give theoretical and numerical analyses of the stability conditions of both the primary and secondary relaxation channels in rational polygons.

III. ORBIT DECAY IN POLYGONS

We deal with rational polygons of m equal sides, denominated as m-gons, circumscribed below a circle of radius R. The mean collision time $\tau_{cm}=(\pi R/2)\cos(\pi/m)$ and the mean escape time $\tau_{em}=(\pi R^2 m/2\Delta)\sin(2\pi/m)$ can be found on the basis of Eq. (1) with the help of area $A_m=(mR^2/2)\sin(2\pi/m)$ and perimeter $P_m=2mR\sin(\pi/m)$. In the limit $m\to\infty$ one naturally arrives at the circle geometry of the ∞-gon with the mean times $\tau_{c\infty}=\tau_{cR}^{(CB)}=\pi R/2$ and $\tau_{e\infty}=\tau_{eR}^{(CB)}=\pi^2R^2/\Delta$, both characteristic of the CB. This demonstrates how average dynamic characteristics can be introduced through the aforementioned geometrical correspondence that takes place between the ∞-gon and the CB. In view of the vertex-memory effects, which forbid interchange between of the temporal ($t\to\infty$) and spatial ($m\to\infty$) limits, the dynamical correspondence does not exist [17].

A. Small numbers of vertices

Similar to the closed m-gons [17], let us consider the case of a small numbers of vertices, $m<10$, in the context of the deterministic approach to the regular-orbit description [16]. This is straightforwardly given by the fact that the wall-collision angles φ (defined with respect to the normal to the piecewise-linear boundary and preserved by elastic refections) are integrals of motion, as is true for complete integrable billiards. Such a description of regular-orbit motion in rational polygons is introduced accounting for the observation [40] that m (or $m/2$) sides of a given m-gon, with odd (or even) number of vertices, are dynamically equivalent. The wall-collision statistics for regular orbits with a fixed collision-angle φ can therefore be reduced to the interval $\varphi=[0,\varphi_m]$, where

$$\varphi_m=\begin{cases}\pi/2m & \text{for odd } m\\ \pi/m & \text{for even } m.\end{cases} \tag{4}$$

The regular orbits with a given φ are thereby distinguished through the φ-orbit characteristic collision times, namely,

$$t_{cm}(\varphi)=\frac{\pi R}{2}\frac{\sin(\varphi_m)\cos(\pi/m)}{\varphi_m\cos(\varphi-\psi_m)}, \tag{5}$$

with

$$\psi_m=\begin{cases}0 & \text{for odd } m \text{ and } m/2\\ \pi/m & \text{for even } m/2,\end{cases} \tag{6}$$

(see the Appendix for details). The φ-orbit collision time is related to the billiard mean collision time τ_{cm} through the mean-collision-time equation, namely,

$$\langle t_{cm}(\varphi)\rangle_c\equiv\int_0^{\varphi_m}t_{cm}(\varphi)f_{0m}(\varphi)d\varphi=\tau_{cm}, \tag{7}$$

which is equivalent to the mean-free-path equation [19]. Equation (7) was considered [16,19,26] in the uniformly populated *wall-collision* space Ω_{cm}, which is 2D subspace of the 3D phase space Ω_m. The φ-orbit distribution function, namely,

$$f_{0m}(\varphi)=\begin{cases}\dfrac{\cos(\varphi-\psi_m)}{\sin(\varphi_m)} & \text{for space } \Omega_{cm}\\ \dfrac{t_{cm}(\varphi)}{\tau_{cm}}\dfrac{\cos(\varphi-\psi_m)}{\sin(\varphi_m)}\equiv\dfrac{1}{\varphi_m} & \text{for space } \Omega_m\end{cases} \tag{8}$$

is defined in Eq. (7) and found here via generalization of Eqs. (6) and (7) in Ref. [16].

Let us discuss the late-time ($t\gg\tau_{em}$) survival dynamics in a given m-gon through (i) the φ-orbit decay spectra presented by the partial-orbit numbers $\mathfrak{N}_m(t,\varphi)$ and (ii) the corresponding total-orbit numbers $N_m(t)$ of survived initial particles $N_m(0)$. The universal relaxation channel, associated with regular orbits, is described by the late-time evolution of nonescaped orbits, predicted by the leading asymptotic terms of Eq. (3), adapted for nonchaotic open billiards [16] and represented here for m-gons, namely,

$$\frac{\mathfrak{N}_m(t,\varphi)}{N_m(0)}=C_m(\varphi)\frac{t_{cm}(\varphi)}{\tau_{cm}}f_{0m}(\varphi)\frac{\tau_{em}}{t} \text{ and } \frac{N_m(t)}{N_m(0)}=D_m\frac{\tau_{em}}{t}. \tag{9}$$

The partial-orbit and overall-orbit *amplitudes* of α relaxation denoted, respectively, by $C_m(\varphi)$ and D_m in Eq. (9) can be measured directly and found analytically in an explicit form within a certain coarse-grained scheme [15,16]. On the other hand, the main regular-orbit dynamic characteristics, such as aforegiven $t_{cm}(\varphi)$, $f_{0m}(\varphi)$, and τ_{cm}, are common to both the decay and intrinsic dynamics. By employing a condition of self-consistency $\langle\mathfrak{N}_m(t,\varphi)\rangle_c=N_m(t)$, which follows from Eqs. (9) with the help of Eq. (7), one therefore introduces the constraint imposed on the primary-relaxation, regular-orbit amplitudes through the *α-amplitude equation*: $\langle C_m(\varphi)\rangle_c\equiv C_{cm}=D_{cm}$. For the integrable CB of radius R, this equation was experimentally justified [16], i.e., $C_{cR}^{(\exp)}=D_{cR}^{(\exp)}=0.210\pm0.004$ was established with an accuracy limited by a typical statistical error of $\pm2\%$ (see Table 2 in

Ref. [16] for the CB data). In view of vertex-splitting effects, which violate the property of integrability [4], one should expect the violation of the α-amplitude equation in polygons, i.e., $C_{cm}^{(\exp)} \neq D_{cm}^{(\exp)}$ observed within experimental accuracy.

We have performed numerical experiments [41] on decay dynamics in m-gons with small numbers of vertices: $m = 3,4,\ldots,8$. Initially, the particles $[N_m(0) = 10^6]$ were distributed randomly within the two distinct phase spaces Ω_{cm} and Ω_m described in Eq. (8), and then allowed to escape through a small opening Δ ($\ll R$). The condition $\tau_{em} = 300$ was used for all m with the help of Eq. (1). For $m \leqslant 8$, the late-time algebraic decay with $\delta_m = \alpha = 1$ is observed [42] within typical temporal windows given by, approximately, $10\tau_{em} < t \leqslant 10^3 \tau_{em}$. The observed decay spectra are exemplified by the pentagon and the heptagon in Fig. 1. In general, the overall-orbit late-time decay in m-gons with small numbers of vertices shows no noticeable deviation from the primary relaxation [43] (see the left inset in Fig. 1). Thus, the φ-orbit amplitudes $C_m^{(\exp)}(\varphi)$ are derived from the observed numbers $N_m^{(\exp)}(t,\varphi)$ through Eq. (9), accounting for the estimated φ-orbit distribution function $f_{0m}(\varphi)$ and collision times $t_{cm}(\varphi)$ given in, respectively, Eqs. (4) and (5). Furthermore, $t_{cm}(\varphi)$ was tested experimentally [40] for different m (see, e.g., the right inset in Fig. 1).

The observed partial amplitudes (weights) $C_m^{(\exp)}(\varphi)$ of the slow primary relaxation are analyzed in Fig. 1. As seen, they exhibit regular (small) and irregular (large) deviations from the mean magnitude $C_{cm}^{(\exp)} = C_{cm}^{(\mathrm{tot})}$ indicated by a solid horizontal line. The latter and the regular-orbit amplitudes $C_{cm}^{(\mathrm{reg})}$ [evaluated as averaged $C_m^{(\exp)}(\varphi)$ without regard to the large isolated peaks] are accumulated in Table I. From an analysis of the deviations for the overall ΔD_{cm} $(= D_{cm}^{(tot)} - D_{cm}^{(\mathrm{reg})}$, with $D_{cm}^{(\mathrm{reg})} = C_{cm}^{(\mathrm{reg})})$ and average partial amplitudes ΔC_{cm} $(= C_{cm}^{(\mathrm{tot})} - C_{cm}^{(\mathrm{reg})})$, obtained with the help of Table I, one can see that the vertex-splitting effects in the even-gons are more pronounced than those in the odd gons, similar to the case of intrinsic dynamics [17]. The α-amplitude deviations ΔC_{cm} and ΔD_{cm} exceed considerably the typical experimental error ($\pm 2\%$) and achieve a maximum magnitude of 30% in the heptagon. This implies that the irregular-orbit motion is substantially involved in the observed late-time primary relaxation that, similar to the integrability, violates the α-amplitude equation [43]. On the other hand, the positive sign of all the α-amplitude deviations signals on effective enhancement of the primary relaxation related solely to regular orbits. The observed effect in vertex-splitting m-gons with $3 \leqslant m \leqslant 8$ is similar to the enhanced diffusion established [17] through the diffusion exponent $1 \leqslant z_m \leqslant 3/2$, which also achieves a maximum at $m = 7$. We associate, therefore, the enhanced decay and diffusion with stabilization of nonballistic regime, which is due to some unspecified orbits whose collision angles are given by large peaks in Fig. 1.

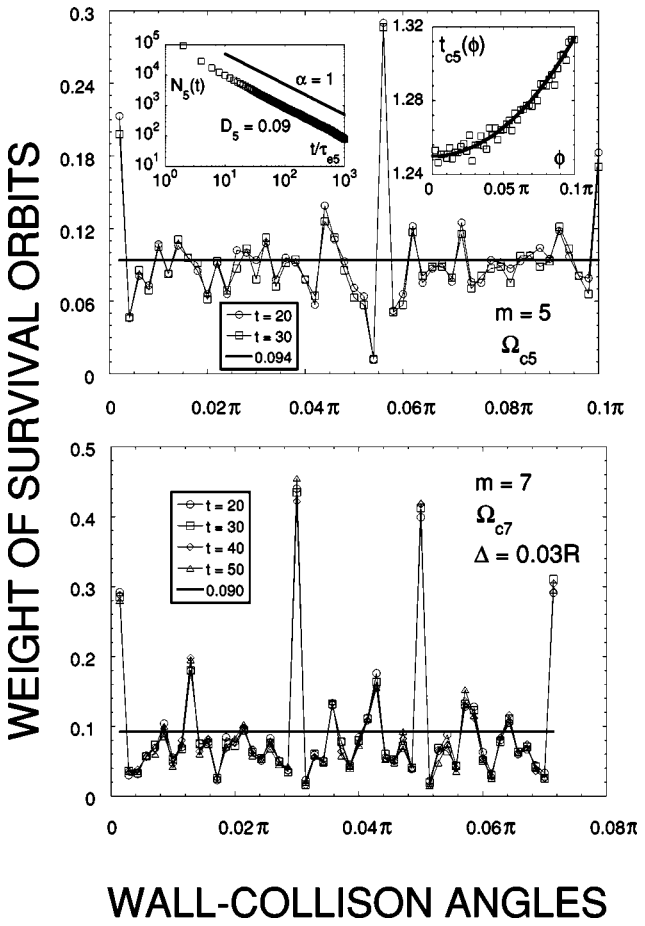

FIG. 1. Analysis of the late-time algebraic decay simulated in the collision Ω_{cm} space of the pentagon ($m = 5$) and the heptagon ($m = 7$). Symbols represent numerical data on the α-relaxation φ-orbit amplitudes (weights) $C_5^{(\exp)}(\varphi)$ and $C_7^{(\exp)}(\varphi)$ deduced from the observed spectra of the survived φ-orbits $N_{t5}^{(\exp)}(\varphi)$ $[\equiv \mathfrak{N}_5^{(\exp)}(t,\varphi)]$ and $N_{t7}^{(\exp)}(\varphi)$ with the help of Eq. (9) and simulated at distinct times $t = 20,30\tau_{em}$, with $\Delta = 0.03R$. Line: the overall-collision-angle amplitude $C_{cm}^{(\exp)}$. Inset left: Points represent data on N_{t5} for the survived total orbits at late times and their analysis with the help of Eq. (9). Inset right: Points represent data on φ-orbit collision time $t_{c5}(\varphi)$ simulated within the basic domain $0 \leqslant \varphi \leqslant \pi/10$. Line represents the same predicted in Eq. (5).

B. Large numbers of vertices

The universal two-step relaxation scenario that follows from Eq. (3) is shared by m-gons with arbitrary numbers of vertices. For large $m = 2^n$ with $n = 3,4,\ldots,6$, a crossover from the universal exponential decay to universal ($\alpha = 1$) and nonuniversal ($\beta_m > 1$) algebraic decay regimes are exemplified in Figs. 2 and 3 for the relatively small and large opening widths Δ, respectively. Decay dynamics was simulated [41] for two initial states Ω_m and Ω_{cm} given by the corresponding phase spaces in Eq. (8). No secondary relaxation is found [42] in the wall-collision space case, resembling nonchaotic systems [16], when particles are injected [41] from a polygonal wall. This may be attributed to some unspecified vertex-splitting effects in the Ω_{cm} space, which produce orderlike motion for all m and just enhance primary relaxation. As seen from Figs. 2 and 3, Ω_m spaces with $m > 8$ exhibit secondary relaxation manifested by the algebraic-decay exponents $\beta_m > 1$, which are characteristic for the chaotic BB [24] and SB [20,31,32]. Ω_m decay dynamics, unlike

TABLE I. Fitting parameters for the algebraic-decay amplitudes of primary relaxation of the collision space Ω_{cm} simulated in the weakly open m-gons with $\Delta=0.05R$. Notations: $C_{cm}^{(\mathrm{tot})}$ and $C_{cm}^{(\mathrm{reg})}$ correspond to the average data on the φ -orbit amplitudes $C_{cm}^{(\mathrm{exp})}(\varphi)$ observed in the decay spectra (see Fig. 1) and averaged over, respectively, all the collision angles φ and those with excluding singular-orbit angles manifested by the high peaks; $D_{cm}^{(\mathrm{tot})}=D_{cm}^{(\mathrm{exp})}$- the overall-orbit amplitudes of the algebraic decay given in Eq. (9) and derived within the primary-relaxation observation window (see the left inset in Fig. 1).

m	$C_{cm}^{(\mathrm{tot})}$	$C_{cm}^{(\mathrm{reg})}$	$D_{cm}^{(\mathrm{tot})}$
3	0.140	0.116	0.135
4	0.220	0.219	0.210
5	0.094	0.086	0.090
6	0.149	0.139	0.150
7	0.092	0.069	0.090
8	0.099	0.096	0.100

its intrinsic dynamics treated in terms of the diffusion exponent z_m [17], moves away from that exhibited by the geometrically corresponding CB, with increasing number of vertices m. In the particular case of $\Delta=0.05R$, shown in Fig. 2, the universal relaxation remains stable until $m=64$, but when $m\geqslant m_{\alpha}^{(\mathrm{exp})}=128$ the primary-relaxation observation window becomes closed. The regular-orbit relaxation affected by vertices is assumably transformed into a *singular-orbit* chaoticlike relaxation indicated by the dynamic decay exponent $\beta_m\approx 1.2$. Qualitatively, the same follows from Fig.

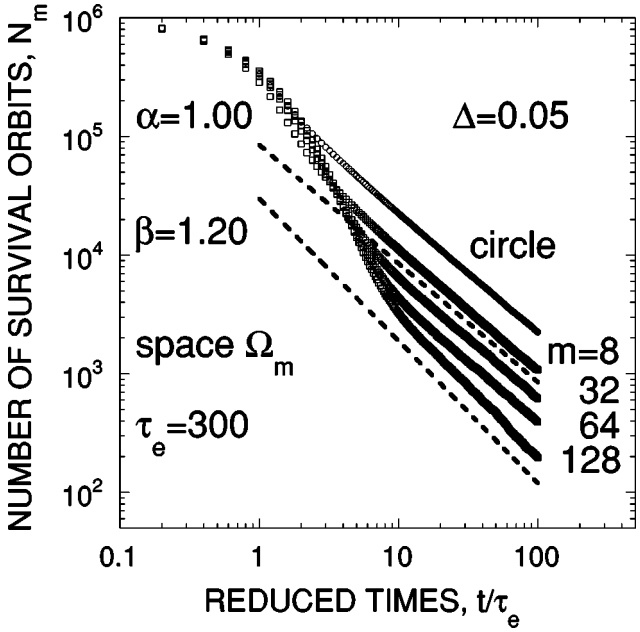

FIG. 2. Temporal evolution of the survived orbits in rational polygons with a small opening width $\Delta=0.05R$ in log-log coordinates. Reduced times are given through the escape characteristic time $\tau_e=300$, chosen common for all cases with the help of Eq. (1). Points: numerical data for the decay of the Ω_m space phase simulated by $N_m(0)=10^6$ particles in m-gons (squares) and the correspondent CB (circles).

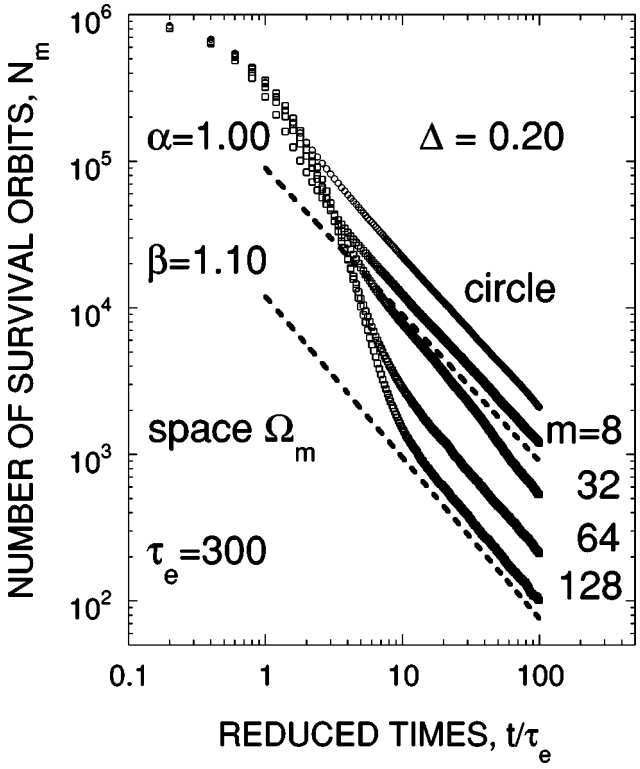

FIG. 3. Temporal evolution of the survived orbits in rational polygons with a large opening width $\Delta=0.20R$ in log-log coordinates. Notations are the same as in Fig. 2.

3, but the upper limit for the α-channel-observation window shows sensitivity to Δ, because $m_{\alpha}^{(\mathrm{exp})}=32$ for $\Delta=0.20R$. We deduce that primary relaxation dominates in the Ω_m space with $3\leqslant m<m_{\alpha}^{(\mathrm{exp})}$, when regular-orbit decay motion is established with the universal decay exponent $\delta_m=\alpha=1$.

It is worth noting that the universal decay relaxation in m-gons with $m<m_{\alpha}^{(\mathrm{exp})}$ can be related to the *universal intrinsic relaxation* in the closed infinite-horizon SB (of side L and scatterer disk radius R). This superdiffusive relaxation was established by the R -independent diffusion exponent $z_R=3/2$ observed for $R<R_{\alpha}$ [33], where $R_{\alpha}=\sqrt{2}L/4$ (see Fig. 2 in Ref. [17]). In the Ω_R space of the corresponding LG, this universal relaxation is due to free evolution of unbounded trajectories along all possible basic corridors [33], which remain open until $R<R_{\alpha}$. Recently, this D-independent intrinsic dynamics was discovered [44] in the 3D Hamiltonian models, lattice Coulomb gas, and *XY*. As shown in Ref. [44], the case of the critical superdiffusive dynamics with $z^{(\mathrm{crit})}=3/2$ is due to a divergent behavior of spatial correlations generated by topological defects, which have the form of *vortex loops*. In closed rational polygons, the vortexlike-orbit relaxation seems to be attributed to the heptagon, but the vortexlike excitations do not survive [17] with the increasing of numbers of sides m. This is not the case of weakly open m-gons with $m>m_{\alpha}^{(\mathrm{exp})}$, whose decay dynamics may be related to nonuniversal intrinsic diffusive relaxation, also observed [17] in the infinite-horizon SB with $R>R_{\alpha}$, when most Bleher's basic corridors are closed.

Similar to the universal-nonuniversal-relaxation crossover in the chaotic SB with $R \approx R_\alpha$, the α-to-β-relaxation crossover in m-gons with $m \approx m_\alpha^{(\exp)}$, is due to a transformation of the motion induced by regular segments of boundary into that by singular. In general, the effect of closing of the α-relaxation channel can be described through the closing of some principal corridors in the Ω_m space. This can be qualitatively understood in terms of the increasing difficulty, as m grows, in realizing long segments of free motion, which intersect polygonal sides in the corresponding LG lattice but avoid the vertex angles (see the Appendix). In contrast, β relaxation is associated with a stabilization in Ω_m phase space of singular-orbit trajectories, which are effectively modified by vertices in rational polygons. These two complete regimes, revealed in the late-time relaxation, are associated with long-lived orbits ensured by the integrals of motion of the 2D classical m-gons, which possesses translational [45] and m-fold rotational symmetries.

Exploration of translational periodicity in m-gons with large m provides characteristic time $t_{cm}(\varphi) \approx \tau_{c\infty} \cos^{-1}(\varphi)$ for any regular orbit with initial collision angle φ, where $\tau_{c\infty} = \pi R/2$. This estimate follows from Eq. (5) and shows that the *idealsliding orbits*, defined [17] by $\varphi \approx \pi/2$ (as circles circumscribed below a given m-gon), leave the piecewise-linear part of boundary. Real sliding orbits, with finite collision times $\tau_{cm}^{(\text{slide})}$, can therefore be introduced as marginal regular orbits given by maximum collision angles $\varphi_m^{(\text{slide})} = \varphi_m$, i.e., with $\tau_{cm}^{(\text{slide})} = t_{cm}(\varphi_m)$. Conversely, the *ideal vortex orbits* are those which slide along the piecewise-linear part of the boundary without reflection. They can be introduced formally by collision angles $\Phi_m/2$, where Φ_m are rational vertex angles. In view of m-fold rotational symmetry, the existence of the real singular-orbit *vortexlike excitations* might be justified by the local preservation of angular momentum for a certain set of vertex-correlated sliding orbits. We therefore assume that the real long-lived sliding (regular) orbits are precursors of the vortexlike (singular) orbits, and the α-to-β-relaxation crossover can be treated in terms of the regular-to-singular orbit transformation that occurs at large numbers $m_\alpha^{(\exp)}$.

Let us consider the m-gon of side length $L_m = P_m/m$, with a small opening of a width Δ ($\ll P_m$) that can be located at any point of the boundary [24,42]. The observation conditions for two distinct *ideal regimes* driven by the ideal sliding and vortex orbits can be introduced as follows. The favorable survival conditions for the α-relaxation regime, induced by regular part of boundary, should exclude vertex-angle effects under the constraint $m < m_\alpha$. A geometrical condition, at which the ideal vortices effectively escape from the billiard table, corresponds to the location of the opening with the width $\Delta \ll L_m$ at one of the vertices. Conversely, in the late-time β-relaxation regime regular orbits do not survive when any side is included into the opening, i.e., when $\Delta \gg L_m$, with $m > m_\alpha$. Hence, the α-to-β crossover relaxation is ensured by the condition $\Delta = L_m$ at $m = m_\alpha$. Taking into account that the perimeter $P_m = 2mR \sin(\pi/m)$ in m-gons with a large number of sides is well approximated by $P_m = 2\pi R$, one arrives at the desirable criterion for α-to-β crossover, namely,

$$m_\alpha = \frac{2\pi R}{\Delta}. \tag{10}$$

The criterion provides the estimates $m_\alpha = 126$ and 31 for experimental data $m_\alpha^{(\exp)} = 128$ and 32, respectively. This finding collaborates the idea that the observed long-lived vortexlike excitations in β relaxation are due to modified sliding orbits. Furthermore, their observation window ($m > m_\alpha$) of chaoticlike excitations disappears in the limit $\Delta \to 0$. This follows from Eq. (10) and was experimentally observed in Ref. [17].

IV. SUMMARY AND CONCLUSIONS

The mild discontinuities caused by vertex angles and relative lengths of edges is the central problem of the intrinsic dynamics of the almost integrable polygonal billiards commonly discussed [1] in terms of orbital ergodicity, mixing, entropy, coding, complexity [6], pseudointegrability [3], orbit-length [14] and quantum-level [10,11] statistics, and orbit-collision statistics [17]. The problem is now related to the decay dynamics in m-gons, studied by the orbit survival probability $S_m(t) = N_m(t)/N_m(0)$, given through the total numbers of the surviving orbits $N_m(t)$. The regular-orbit decay spectra, which avoid vertex-splitting events and therefore preserve a collision angle φ, are also analyzed in terms of the partial-orbit numbers $\mathfrak{N}_m(t,\varphi)$.

A general approach to the decay problem based on a fundamental decay kinetic equation [15,16] naturally arrives at the primary slow relaxation of regular orbits with asymptotic behavior $S_m^{(\alpha)} \propto t^{-1}$ [follows from Eq. (9)]. We have demonstrated that the α channel of relaxation, attributed to both chaotic and nonchaotic billiards, is also characteristic of nonintegrable rational polygons. The universal primary relaxation, experimentally justified by the algebraic decay exponent $\delta_m = \alpha = 1$, is associated with regular orbits originating in the piecewise-linear segments of the polygonal boundary. In the corresponding phase space, under condition $m < m_\alpha$, these orbits are unbounded trajectories along which particles move without splitting at vertices. This relaxation reflects on another universal *intrinsic* relaxation discovered [17] in the chaotic SB with a small disk ($R < R_\alpha$) and ensured [33] by superdiffusive motion along Bleher's basic corridors, with the critical [44] diffusion exponent $z_R = z^{(cr)} = 3/2$.

Following the simplified polygonal orbit classification by Gutkin [1], the regular orbits are presented by the "infinite-past-to-infinite-future" trajectories, which exhibit a regular behavior in the observed m-gon orbit-decay spectra given by $\mathfrak{N}_m^{(\exp)}(t,\varphi)$. Conversely, the singular orbits caused by the "infinite-past-to-vertex," the "vertex-to-infinite-future," and the "vertex-to-vertex" trajectories expose pronounced (partial) amplitudes in the primary relaxation in m-gons with a small number of vertices ($3 \leqslant m \leqslant 8$). As shown through the statistical analysis of the partial and overall amplitudes observed in the spectra $\mathfrak{N}_m^{(\exp)}(t,\varphi)$ and $N_m^{(\exp)}(t)$, the singular orbits violate the α-relaxation amplitude equation, expected

from the absent or weak vertex-splitting effects. Unlike the asymptotic behavior of the orbit-length spectrum [14], the universal primary relaxation therefore exhibits distinctive features in completely integrable and almost-integrable billiards. In the latter case of rational polygons, a nonballistic motion induced by vertices gives rise to enhanced decay and diffusion [17], respectively, in open and closed m-gons with a small number of vertices, m. For a large number of sides $(8<m<m_\alpha)$, the primary slow relaxation is due to the orderlike motion of the long-lived sliding orbits, which possess the largest collision angles.

The sliding orbits are marginal regular orbits and are therefore precursors of the singular, vortexlike-orbit chaotic excitations, which become stable at a very large number of vertices, $m>m_\alpha$. The vortex excitations are established through the slow nonuniversal secondary relaxation with the survival probability $S_m^{(\beta)}\propto t^{-\beta_m}$. They are due to late-time vertex-angle-correlation effects ensured by the m-fold rotational symmetry of a rational polygon. The domain for the decay exponent, i.e., $1<\beta_m<2$, corresponds to that known for the chaotic SB [20,31,32] and BB [24], and the survival probability function $S_m^{(\beta)}$ can therefore be related [46] to the corresponding waiting-time probability function discussed [47] in the theory of open classical chaotic systems. Furthermore, by accounting for the findings of the SB decay dynamics by Fendrik and co-workers [31,32], one can infer that the secondary relaxation is due to the *singular trapped* orbits that move freely along Bleher's reduced basic corridors. Similar to chaotic billiards, and unlike the case of α relaxation, the observation conditions for β relaxation in rational polygons are shown to be sensitive to initial phase-space conditions and to geometrical constrains. Indeed, the β-relaxation channel turns out to be closed if the particle initial distribution is simulated [42] in the collision space Ω_{cm}. In the case of the Ω_m space, the secondary relaxation appears to be stable under the geometrical constraint $m>m_\alpha$, where $m_\alpha=2mR\sin(\pi/m)/\Delta$ is established by the α-to-β crossover-relaxation criterion. This criterion joins survival conditions for the ideal regular-orbit motion with those for the ideal singular-orbit motion generated, respectively, by piecewise-linear and the vertex-angle boundary segments. Finally, we have demonstrated through nonuniversal slow relaxation that the vertex-splitting effects in rational polygons are dual with respect to vertex-ordering and vertex-disordering effects.

ACKNOWLEDGMENTS

The authors are grateful to Josef Klafter for drawing their interest to the escape problem in chaotic systems [47]. Special thanks are due to Mario Jorge Dias Carneiro and Ronald Dickman for numerous stimulating discussions and critical comments. The financial support of the Brazilian agency CNPq is also acknowledged.

APPENDIX: REGULAR-ORBIT COLLISION TIME

In a given m-gon the number of geometrically equivalent walls k is bounded above by

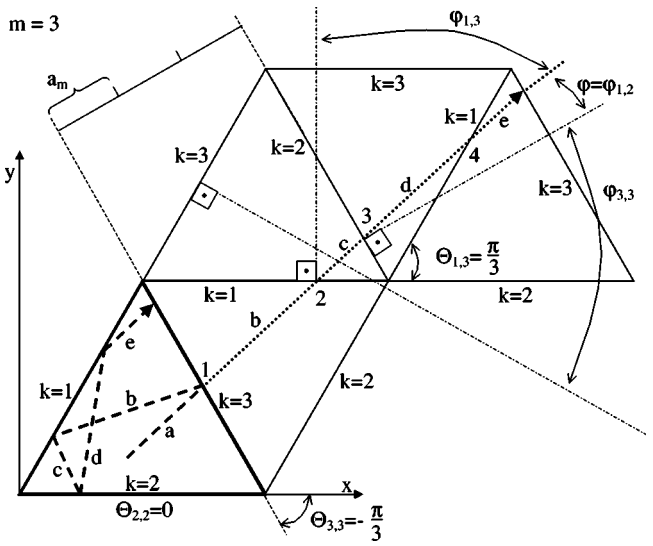

FIG. 4. Estimation of the φ-orbit collision time $t_{cm}(\varphi)$ on the bases of Eq. (A3) for the case of $m=3$. The regular piecewise-linear orbit $a,b,c,\ldots$ is represented by the infinite straight-line trajectory in the triangle LG lattice with the intersection-point sequences $1,2,\ldots,n$ (t,φ_{km}). The equivalent walls k, the unreduced collision angles φ_{km}, and the axillar angles Θ_{km} are shown.

$$q_m=\begin{cases} m & \text{for odd } m \\ m/2 & \text{for even } m. \end{cases} \tag{A1}$$

The current collision angle φ_{km} with a wall k $(=1,2\ldots q_m)$ of a φ-orbit with $\varphi=[0,\pi/2q_m]$ is reduced through the relation $\varphi_{km}=\varphi-\Theta_{km}$ with the help of $\Theta_{km}=[-\pi/2,\pi/2]$, defined as the smallest angle between the k-wall and x axis, namely,

$$\Theta_{km}=\frac{\pi}{2q_m}\begin{cases} q_m-2k+1 & \text{for odd } q_m \\ q_m-2k & \text{for even } q_m. \end{cases} \tag{A2}$$

As exemplified in Fig. 4 for $m=3$, the estimates for the wall-collision times $t_{cm}(\varphi)$ are found through summation of the numbers of intersections $n(t,\varphi_{km})$ for a trajectory induced by a given φ-set orbit in the corresponding infinite LG lattice, namely,

$$n_{cm}(t,\varphi)\equiv\frac{t}{t_{cm}(\varphi)}=\sum_{k=1}^{q_m} n(t,\varphi_{km}). \tag{A3}$$

This estimation procedure can be exemplified by a relation $t\cos(\varphi_{13})=n(t,\varphi_{13})3a_3$. The latter employes the fact that a distance between the equivalent walls is $3a_3$, where $a_m=R\cos(\pi/m)$ stands for the *apothem* in a given m-gon. This yields

$$t_{cm}(\varphi)=a_m q_m\left[\sum_{k=1}^{q_m}\cos(\varphi-\Theta_{km})\right]^{-1}, \tag{A4}$$

where q_m and Θ_{km} are given in Eqs. (A1) and (A2), respectively. A straightforward estimation [45] of Eq. (A4) results in the collision time $t_{cm}(\varphi)$ given in Eq. (5).

[1] E. Gutkin, J. Stat. Phys. **83**, 7 (1996).
[2] A.N. Zemlyakov and A.B. Katok, Math. Notes (Leipzig) **18**, 760 (1975).
[3] P.J. Richens and M.V. Berry, Physica D **2**, 495 (1981).
[4] B. Echardt, J. Ford, and F. Vivaldi, Physica D **13**, 339 (1984).
[5] E. Gutkin, Physica D **19**, 311 (1986).
[6] G. Mantica, Phys. Rev. E **61**, 6434 (2000).
[7] Y.G. Sinai, Russ. Math. Surveys **25**, 137 (1979).
[8] L.A. Bunimovich, Commun. Math. Phys. **65**, 295 (1979).
[9] J.L. Vega, T. Uzer, and J. Ford, Phys. Rev. E **48**, 3414 (1993).
[10] T. Cheon and T.D. Cohen, Phys. Rev. Lett. **62**, 2769 (1989).
[11] A. Shudo and Y. Shimizu, Phys. Rev. E **47**, 54 (1993).
[12] Y. Shimizu and A. Shudo, Chaos, Solitons Fractals **5**, 1337 (1995).
[13] F. Henyey and N. Pomphrey, Physica D **6**, 78 (1982).
[14] A. Shudo, Phys. Rev. A **46**, 809 (1992).
[15] V.B. Kokshenev and M.C. Nemes, Physica A **275**, 70 (2000).
[16] E. Vicentini and V.B. Kokshenev, Physica A **295**, 391 (2001).
[17] V.B. Kokshenev and E. Vicentini, Phys. Rev. E **65**, 015201(R) (2002).
[18] R.W. Robbinett, J. Math. Phys. **40**, 101 (1999).
[19] P.L. Garrido and G. Gallavotti, J. Stat. Phys. **76**, 549 (1994).
[20] R. Artuso, G. Casati, and I. Guarneri, J. Stat. Phys. **83**, 145 (1996).
[21] J. Machta and R. Zwanzing, Phys. Rev. Lett. **50**, 1959 (1983).
[22] B. Freidman and R.F. Martin, Phys. Lett. A **105**, 23 (1984).
[23] A. Zacherl, T. Geisel, J. Nierwetberg, and G. Radons, Phys. Lett. A **114**, 317 (1986).
[24] H. Alt, H.-D. Gräf, H.L. Harney, R. Hofferbert, H. Rehfeld, A. Richter, and P. Schardt, Phys. Rev. E **53**, 2217 (1996). It was etablished experimentally that a position of the opening, unlike its width Δ, does not affect the geometrically dependent decay exponents $\beta=\delta>1$.
[25] F. Vivaldi, G. Casati, and I. Guarneri, Phys. Rev. Lett. **51**, 727 (1983).
[26] N. Chernov, J. Stat. Phys. **88**, 1 (1997).
[27] P.L. Garrido, J. Stat. Phys. **88**, 807 (1997).
[28] W. Bauer and G.F. Bertsch, Phys. Rev. Lett. **65**, 2213 (1990).
[29] L.A. Bunimovich, Sov. Phys. JETP **62**, 842 (1985).
[30] A.S. Pikovsky, J. Phys. A **25**, L477 (1992).
[31] A.J. Fendrik, A.M.F. Rivas, and M.J. Sánchez, Phys. Rev. E **50**, 1948 (1994). When bouncing-ball trajectories are excluded by special escape conditions, only a pure exponential decay is observed.
[32] A.J. Fendrik and M.J. Sánchez, Phys. Rev. E **51**, 2996 (1995).
[33] P.M. Bleher, J. Stat. Phys. **66**, 315 (1992).
[34] P. Dahlqvist, J. Stat. Phys. **84**, 773 (1996).
[35] C.F. Hillermeier, R. Blümel, and U. Smilansky, Phys. Rev. A **45**, 3486 (1992).
[36] It was recently claimed by N. Friedman *et al.*, in Phys. Rev. Lett. **86**, 1518 (2001) that solely exponential decay is attributed to the ''real'' atom-optics ''titled''-stadium-shaped billiard. No explanations were given for why the late-time decay regime, controlled by the boundary hole through the observation window, was not achieved.
[37] R. Dickman and D. ben-Avaraham, Phys. Rev. E **64**, 020102(R) (2001).
[38] R. Dickman, F.F. Araujo, Jr., and D. ben-Avaraham, Phys. Rev. E **66**, 051102 (2002).
[39] L.A. Bunimovich and Ya.G. Sinai, Commun. Math. Phys. **78**, 479 (1981).
[40] Taking into account that the vertex angles in a m-gon are given by $\Phi_m=\pi(1-2/m)$, one can see that any orbit is presented by m (or by $m/2$) distinct collision angles for even (or odd) m and, hence, all m (or $m/2$) sides are dynamically equivalent. See also footnote 3 in Ref. [16].
[41] For details of the computer experiment, see Sec. 4 in Ref. [16].
[42] E. Vicentini, Ph.D. dissertation, Universidade Federal of Minas Gerais, Brazil, 2001.
[43] Exception should be made in the case of $m=4$ for which intrinsic dynamics was established in Ref. [16]. The late-time decay dynamics is also due to bouncing-ball orbits, with $\Delta C_c 4=0$ and $\Delta D_c 4<0$ derived from Table I.
[44] P. Minnhagen, B.J. Kim, and H. Weber, Phys. Rev. Lett. **87**, 037002 (2001).
[45] A geometric correspondence between a given m-fold rotational-symmetry polygon and the infinite-range periodically translated LG lattice exists only in the cases $m=3,4$, and 6. One can however show that Eq. (A4) works well for the long-lived orbits when $t\gg a_m q_m$. This follows from the same estimation procedure shown in Fig. 4 and is corroborated by our numerical analysis illustrated in the right inset in Fig. 1.
[46] V.B. Kokshenev and E. Vicentini (unpublished).
[47] G. Zumofen, J. Klafter, and M.F. Shlesinger in *Lecture Notes in Physics*, edited by R. Kutner, A. Pekalski, and K. Sznajd-Weron (Springer, Berlin, 1999), Vol. 519, p. 15.